

# SIRT1 activation enhances HDAC inhibition-mediated upregulation of GADD45G by repressing the binding of NF- $\kappa$ B/STAT3 complex to its promoter in malignant lymphoid cells

A Scuto<sup>\*1</sup>, M Kirschbaum<sup>2</sup>, R Buettner<sup>1</sup>, M Kujawski<sup>3</sup>, JM Cermak<sup>4</sup>, P Atadja<sup>5</sup> and R Jove<sup>1</sup>

We explored the activity of SIRT1 activators (SRT501 and SRT2183) alone and in combination with panobinostat in a panel of malignant lymphoid cell lines in terms of biological and gene expression responses. SRT501 and SRT2183 induced growth arrest and apoptosis, concomitant with deacetylation of STAT3 and NF- $\kappa$ B, and reduction of c-Myc protein levels. PCR arrays revealed that SRT2183 leads to increased mRNA levels of pro-apoptosis and DNA-damage-response genes, accompanied by accumulation of phospho-H2A.X levels. Next, ChIP assays revealed that SRT2183 reduces the DNA-binding activity of both NF- $\kappa$ B and STAT3 to the promoter of GADD45G, which is one of the most upregulated genes following SRT2183 treatment. Combination of SRT2183 with panobinostat enhanced the anti-growth and anti-survival effects mediated by either compound alone. Quantitative-PCR confirmed that the panobinostat in combination with SRT2183, SRT501 or resveratrol leads to greater upregulation of GADD45G than any of the single agents. Panobinostat plus SRT2183 in combination showed greater inhibition of c-Myc protein levels and phosphorylation of H2A.X, and increased acetylation of p53. Furthermore, EMSA revealed that NF- $\kappa$ B binds directly to the GADD45G promoter, while STAT3 binds indirectly in complexes with NF- $\kappa$ B. In addition, the binding of NF- $\kappa$ B/STAT3 complexes to the GADD45G promoter is inhibited following panobinostat, SRT501 or resveratrol treatment. Moreover, the combination of panobinostat with SRT2183, SRT501 or resveratrol induces a greater binding repression than either agent alone. These data suggest that STAT3 is a corepressor with NF- $\kappa$ B of the GADD45G gene and provides *in vitro* proof-of-concept for the combination of HDACi with SIRT1 activators as a potential new therapeutic strategy in lymphoid malignancies.

*Cell Death and Disease* (2013) 4, e635; doi:10.1038/cddis.2013.159; published online 16 May 2013

**Subject Category:** Experimental medicine

Histone deacetylase inhibitors (HDACi) such as panobinostat, which inhibit the zinc containing catalytic domain of HDAC of classes I, II, and IV, demonstrate clinical and preclinical activities against various malignancies, particularly lymphoid malignancies.<sup>1–3</sup> Sirtuin-1 (SIRT1) is an NAD<sup>+</sup>-dependent class III HDAC, which deacetylates histones as well as non-histone proteins and is not affected directly by HDACi, such as panobinostat.<sup>4</sup> Several studies have supported SIRT1 as regulator of diverse physiological functions, including metabolic responses to caloric restriction and exercise training, circadian rhythm, DNA repair, cell survival, senescence, death, and differentiation.<sup>5</sup> A potential role for SIRT1 in diabetes, cardiovascular disease, inflammation, neurodegeneration, and cancer has been demonstrated as well.<sup>5,6</sup> It is unclear whether increasing SIRT1 levels/activity has

beneficial physiological effects or not and whether SIRT1 has tumor suppressor or oncogenic functions.

Although several of the class I, II, and IV HDAC inhibitors are in phase I–III clinical trials,<sup>1–3</sup> currently available SIRT1 inhibitors remain primarily research tools for *in vitro* applications or mouse model studies.<sup>7</sup> Given the range of activity of the currently available HDAC inhibitors, it may be valuable to identify clinically useful SIRT1 inhibitors. Thus, efforts to find either derivatives of known SIRT1 inhibitors or novel SIRT1 inhibitors with higher potency and selectivity are still in progress. However, a couple of SIRT1 activators have been or are underway to be dosed in human trials in type 2 diabetes.<sup>7</sup> It remains controversial whether inhibition of SIRT1 or its activation is more efficacious in anticancer therapy. On the one hand, there is evidence that inhibition of SIRT1 by

<sup>1</sup>Molecular Medicine, Beckman Research Institute, City of Hope Comprehensive Cancer Center, Duarte, CA, USA; <sup>2</sup>Hematological Malignancies, Penn State Hershey Cancer Center, Hershey, PA, USA; <sup>3</sup>Immunology, Beckman Research Institute, City of Hope Comprehensive Cancer Center, Duarte, CA, USA; <sup>4</sup>Sirtris, Cambridge, MA, USA and <sup>5</sup>Novartis Institute for Biomedical Research, Cambridge, MA, USA

\*Corresponding author: Dr A Scuto, Molecular Medicine, Beckman Research Institute, City of Hope Comprehensive Cancer Center, 1500 East Duarte Road, Duarte, CA 91010, USA. Tel: (626) 256-4673; Fax: (626) 256-8708; E-mail: ascuto@coh.org

**Keywords:** HDAC; SIRT1 activators; panobinostat; STAT3; NF- $\kappa$ B; GADD45G

**Abbreviations:** SIRT1, sirtuin-1; HDAC, histone deacetylase; HDACi, histone deacetylase inhibitors; NF- $\kappa$ B, nuclear factor kappa-B; STAT3, signal transducer and activator of transcription 3; GADD45G, growth arrest and DNA-damage-inducible protein gamma; H2A.X, H2A histone family, member X; cDNA, complementary deoxyribonucleic acid; siRNA, small interfering ribonucleic acid; qRT-PCR, quantitative real-time PCR; ChIP, chromatin immunoprecipitation; EMSA, electrophoretic mobility shift assays; MTS, 3-(4,5-dimethylthiazol-2-yl)-5-(3-carboxymethoxyphenyl)-2-(4-sulfophenyl)-2H-tetrazolium inner salt; PI, propidium iodide; ALL, acute lymphoblastic leukemia; ABC, activated B-cell; DLBCL, diffuse large B-cell lymphoma; DMSO, dimethyl sulfoxide; SDS, sodium dodecyl sulfate; PAGE, polyacrylamide gel electrophoresis; IC<sub>50</sub>, median inhibition concentration; CI, combination index

Received 15.11.12; revised 29.3.13; accepted 03.4.13; Edited by A Stephanou

small interfering ribonucleic acid (siRNA) leads to re-expression of tumor-suppressor genes<sup>8</sup> and SIRT1 small molecule inhibitors induce apoptosis in cancer cells associated with increased levels of acetyl-p53.<sup>9</sup> On the other hand, the SIRT1 activator resveratrol, which is a polyphenolic flavonoid present in red wine with potent antioxidant properties, possesses anti-leukemia, anti-lymphoma, and anti-myeloma effects associated with inhibition of signal transducer and activator of transcription 3 (STAT3) and nuclear factor kappa-B (NF- $\kappa$ B) signaling.<sup>10–15</sup>

In the present study, we focused on two novel SIRT1 activators SRT501<sup>16,17</sup> and SRT2183<sup>18</sup> as pharmacological tools to investigate whether they would lead to anti-tumor activity in malignant lymphoid cells cultured *in vitro*. SRT501 is a proprietary formulation of resveratrol with enhanced pharmacokinetic properties and improved oral bioavailability, while SRT2183 is a non-natural product-derived small-molecule SIRT1 activator structurally unrelated to resveratrol. Recent evidence demonstrates that SRT501 and SRT2183 can directly activate SIRT1 through an allosteric mechanism.<sup>19,20</sup> We have previously reported that the anti-tumor activity of the HDAC inhibitor panobinostat in pre-B acute leukemia cells is partly mediated by upregulation of the growth arrest and DNA-damage-response gene, GADD45G, associated with histone hyperacetylation at the promoter level.<sup>21</sup> To our knowledge, there is presently no study that explored the potential mechanism of action of a class I, II, and IV HDAC inhibitor in combination with either a SIRT1 inhibitor or a SIRT1 activator.

Here, a panel of malignant lymphoid cell lines was treated with either the SIRT1 activator SRT501 or the SIRT1 activator SRT2183, as well as in combination with panobinostat, and evaluated for biological and gene expression responses. The rationale behind this study is that while panobinostat exerts its anti-tumor activity partly by leading to re-activation of tumor-suppressor genes associated with acetylation of their promoters,<sup>21</sup> SIRT1 activators may lead to anti-tumor effects via the inhibition of the activity of transcription factors that are substrates of SIRT1 and negative regulators of tumor-suppressor genes. Hence, the combination of a SIRT1 activator with panobinostat may have greater anti-tumor effect. The main purpose of this investigation was to determine whether the combination of a class I, II, and IV HDAC inhibitor with a SIRT1 activator may have potential as a new strategy for therapy of lymphoid malignancies in need of new treatment options.

## Results

**SIRT1 activators, SRT501 and SRT2183, inhibit proliferation and induce apoptosis of human malignant lymphoid cells associated with deacetylation of STAT3 and NF- $\kappa$ B p65.** We investigated the effects of treatment with SRT2183 or SRT501 on a panel of human malignant lymphoid cell lines. We first determined the effect of SRT2183 or SRT501 on the proliferation of two pre-B acute lymphoblastic leukemia (ALL) cell lines, Reh and Nalm-6, which were both sensitive to the HDAC inhibitor panobinostat<sup>21</sup> (Figures 1a and b,

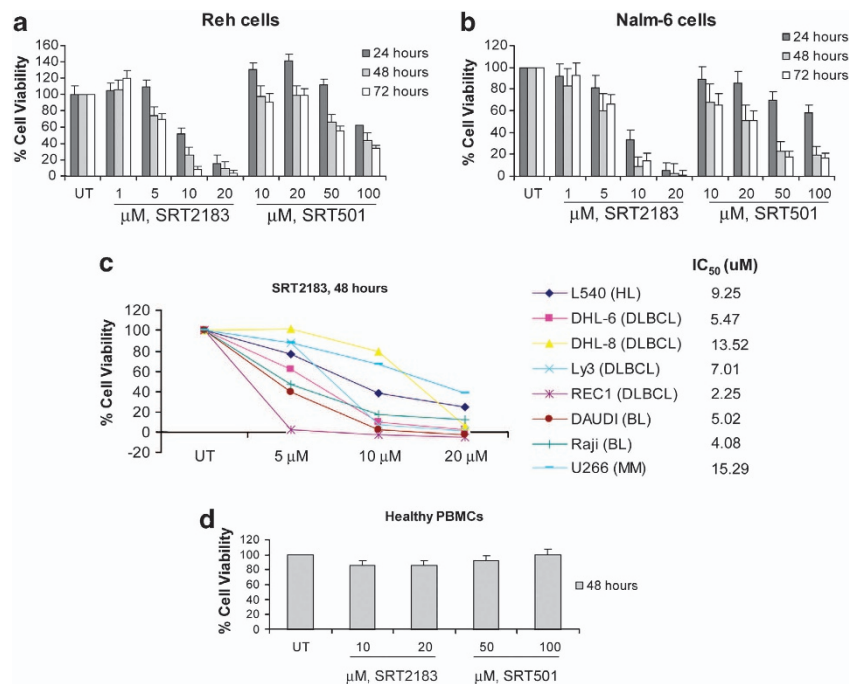


**Figure 1** SIRT1 activators inhibit viability of human malignant lymphoid B-cell lines. (a) Reh cells and (b) Nalm-6 cells were treated with the indicated concentrations of SRT2183 or SRT501 for 24, 48, or 72 h. Following this, the percentage of cell viability was determined by MTS assay. Values represented as graphs are the mean of three independent experiments with S.D. (c) Cells were treated with the indicated concentrations of SRT2183 for 48 h. Following this, the percentage of cell viability was determined by MTS assay. (d) Peripheral blood mononuclear cells from a healthy donor were treated in culture with the indicated concentrations of SRT2183 or SRT501 for 48 h. The percentage of viable cells was determined by DIMSCAN analysis. Values represent the percentages of cell viability normalized to that of the untreated cells and are the mean of three separate treatments

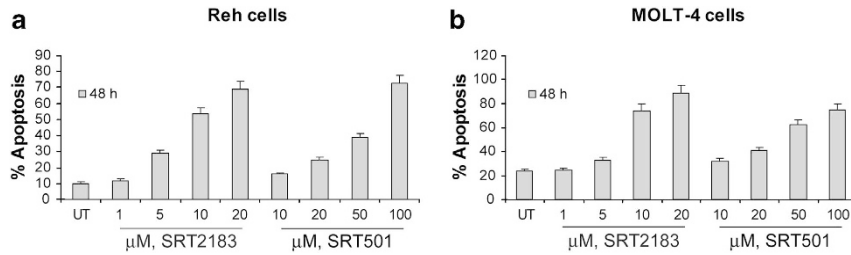


**Figure 2** SIRT1 activators induce apoptosis of human Ph<sup>+</sup> ALL cell lines. (a) Reh cells and (b) MOLT-4 cells were treated with the indicated concentrations of SIRT2183 or SIRT501 for 48 h. Following this, the percentage of apoptotic cells was determined by flow cytometry using Annexin V/propidium iodide staining. Values represented as bar graphs are the mean of three independent experiments with S.D.

respectively). MTS ((3-(4,5-dimethylthiazol-2-yl)-5-(3-carboxymethoxyphenyl)-2-(4-sulfophenyl)-2H-tetrazolium, inner salt) assays showed that both SIRT1 activators markedly inhibit the growth of Reh and Nalm-6 cells in a time- and dose-dependent manner. The data also indicate that SIRT2183 is much more potent than SIRT501 in inhibiting proliferation. The IC<sub>50</sub> (median inhibition concentration) values for SIRT2183-mediated inhibition of proliferation at 48 h are approximately 8.7 μM for Reh cells and approximately 3.2 μM for Nalm-6 cells; in the same cell lines the IC<sub>50</sub> at 48 h for SIRT501 are approximately 94 and 20 μM, respectively. The effect of SIRT2183 on cell proliferation was determined for a wider variety of malignant lymphoid cell lines. Figure 1c shows that SIRT2183 has broad efficacy, with an IC<sub>50</sub> at 48 h ranging from 2 to 15 μM. By contrast, no cytotoxic effects were observed in normal cells at those concentrations that induce strong inhibition of cell viability in tumor cells (Figure 1d).

The apoptotic effect of SIRT2183 or SIRT501 was determined 48 h post treatment in Reh cells as well as in MOLT-4, which is a T-cell ALL cell line also reported to be sensitive to panobinostat<sup>21</sup> (Figures 2a and b, respectively). Exposure to either one of the two SIRT1 activators induces apoptosis of both Reh and MOLT-4 cells in a dose-dependent manner. The IC<sub>50</sub> values in terms of apoptosis are approximately 12 and 8.7 μM for SIRT2183 in Reh and MOLT-4 cells, respectively, and 66 and 53.2 μM for SIRT501 in the same cell lines, respectively.

STAT3 and NF-κB have been validated as SIRT1 substrates.<sup>22–25</sup> It is well established that acetylation at Lys-685 is critical for STAT3 phosphorylation, dimerization, nuclear translocation, and transactivation.<sup>22,26</sup> Moreover, acetylation of p65 NF-κB at Lys-310 is required for its full transcriptional activity.<sup>27</sup> Furthermore, SIRT1 activation by the SIRT1 agonist resveratrol has anti-myeloma, anti-lymphoma, and anti-leukemia effects involving STAT3 and NF-κB activity.<sup>10–15</sup> Thus, we wanted to demonstrate whether SIRT2183 and SIRT501 also had effects in the acetylation status of both STAT3 and NF-κB in the two cell lines that have both these signaling pathways constitutively activated, Reh as well Ly3, an activated B-cell (ABC)-like diffuse large B-cell lymphoma (DLBCL) cell line.<sup>28</sup> The acetylation of both NF-κB and STAT3 is affected in Reh cells (Figure 3a), by either SIRT1 activator. SIRT1 activators did not affect phosphorylation of NF-κB at Ser536 (data not shown), which stimulates acetylation of Lys310 by increasing the assembly with p300.<sup>29</sup> Flow cytometry analysis demonstrated the repression of both total and phospho-STAT3 (Lys705) levels by SIRT501 and SIRT2183 in the Reh cell line (Supplementary Figures S2A

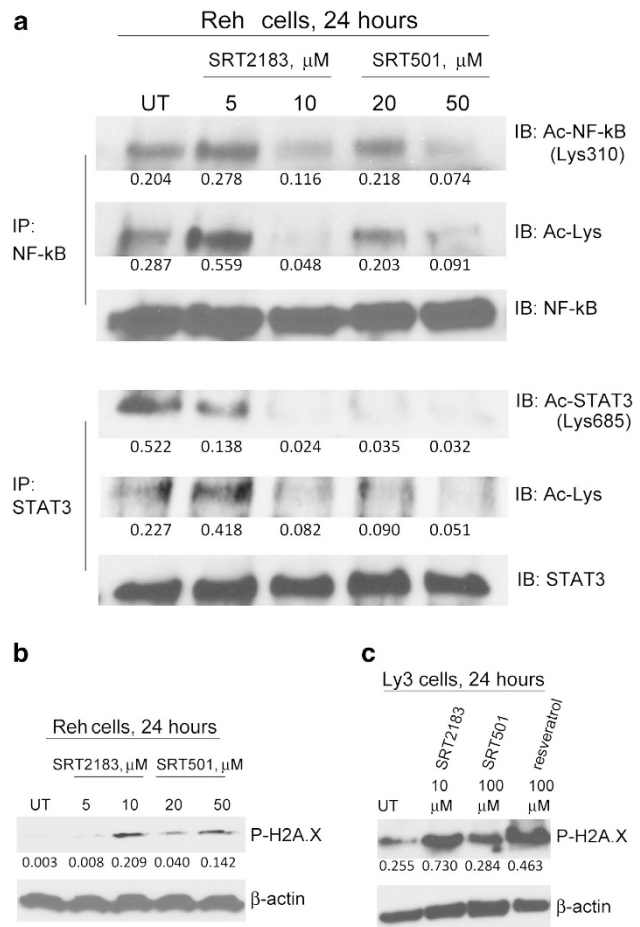


**Figure 3** SIRT1 activators lead to deacetylation of both STAT3 and NF-κB p65 and induce phosphorylation of H2A.X. Cells were treated with the indicated concentrations of SIRT2183 or SIRT501 for 24 h. Following this, (a) immunoprecipitation (IP) and subsequent immunoblotting (IB) were performed on the lysates from Reh cells to analyze acetyl-STAT3 and acetyl-NF-κB levels. The levels of total STAT3 and total NF-κB served as loading controls. Results are representative of three independent experiments. Western blot analysis of phospho-H2A.X protein was performed on the lysates from (b) Reh or (c) Ly3 cells 24 h post treatment. The levels of β-actin protein served as loading controls. Results are representative of three independent experiments

and 2B, respectively). Total STAT3 levels are also diminished due to the autoregulation of the STAT3 promoter. The c-myc gene has been identified as target of STAT3.<sup>30</sup> Moreover, NF-κB and STAT3 are co-dependent and both can regulate the pro-oncogenic transcription factor Myc.<sup>31</sup> We

demonstrated that both SIRT1 activators repress c-Myc protein levels in Reh cells in a dose-dependent manner (Supplementary Figure S2C).

**SRT501 and SRT2183 induce expression of DNA-damage response genes associated with accumulation of phospho-H2A.X levels.** In our previous study,<sup>21</sup> we showed that panobinostat-mediated HDAC inhibition induces upregulation of DNA-damage response and apoptosis-related genes, associated with apoptosis and hyperphosphorylation of H2A histone family, member X (H2A.X), which is associated with DNA-damage response.<sup>32</sup> As among the substrates of SIRT1 there are also transcription factors that function as negative regulators of apoptosis-related genes, we wanted to investigate whether SIRT1 activation induced changes in the expression of a panel of genes involved in DNA-damage response and apoptosis. In Supplementary Table S1, data from PCR array experiments performed in Reh cells are shown for those genes in which the fold upregulation is above 1.95, showing that SIRT1 activator SRT2183 upregulates several genes involved in DNA-damage response and apoptosis. GADD45G was observed to be one of the most upregulated genes after SIRT1 activator treatment. Moreover, we demonstrate that SIRT1 activators induce accumulation of phospho-H2A.X in Reh as well as in Ly3 cells (Figures 3b and c, respectively).

**Combination of SRT2183 with HDAC inhibitor panobinostat enhances the anti-proliferative and anti-survival effects mediated by either compound alone.** Next we wanted to investigate the possible consequences of combining the SIRT1 activators with an HDAC inhibitor selective for class I, II, and IV HDAC. The combination of HDAC inhibitor panobinostat plus SRT2183 induces superior anti-tumor effects in Reh cells than either agent alone (Figure 4). The percentage of cell proliferation inhibition was 5, 40, and 70% when Reh cells were treated with 10 nM panobinostat, 10  $\mu$ M SRT2183, or a combination of both, respectively (Figure 4a). The percentage of total apoptosis induced by 10 nM panobinostat or 10  $\mu$ M SRT2183 was 30% for both single agents and 50% for the combination of them (Figure 4b). In Ly3 cells, we observed similar biological responses in terms of inhibition of viability. Figure 4c shows that Ly3 cells are sensitive to panobinostat and to SRT2183, which inhibits cell viability in a dose-dependent manner. Moreover, the combination of SRT2183 with panobinostat induces greater cell viability inhibition than either compound alone. By contrast, this combination did not affect the viability of human peripheral blood mononuclear cells from a healthy donor (Figure 4d). Combination index (CI) analysis revealed that this enhanced response with combination treatment represents an additive-to-moderate synergistic response ( $0.98 < CI < 0.79$ ).

The combination of panobinostat plus SRT2183 also showed greater inhibition of c-Myc protein levels in all the cell lines tested (Reh, NALM-6, and MOLT-4 cells, Supplementary Figures S3A–3C, respectively), as well as enhanced phosphorylation of H2A.X (Figures 5a and b and Supplementary Figure S3C), greater acetylation of H4 (Figures 5a and b and Supplementary Figure S3C), and

increased acetylation of p53 (acetylation of p53 was not seen with SRT2183 alone) (Supplementary Figures S3A and 3B).

**GADD45G siRNA transfection confers partial protection from SIRT1 activator alone or in combination with panobinostat.** PCR array data demonstrated that GADD45G is one of the most upregulated genes after SIRT1 activator treatment. By quantitative real-time PCR, we confirm that 10  $\mu$ M SRT2183 upregulates GADD45G expression in Reh cells, we also demonstrate that the combination of panobinostat with SRT2183 leads to significantly higher expression of GADD45A and GADD45G than either agent alone in both Reh and Nalm-6 cells (Figures 6a and b, respectively). Boosted upregulation of these genes was observed even combining panobinostat with the lowest doses of SRT2183, which did not show gene upregulation when used alone. We then performed quantitative real-time PCR to evaluate the effect of treatment with SIRT1 activators alone or in combination with panobinostat on GADD45G expression in Ly3 cells. Figure 6c demonstrates that while GADD45G is modestly upregulated in response to panobinostat, SRT501, and resveratrol, the combination of either SIRT1 activator is considerably increased with panobinostat. However, the effect on expression of GADD45G after treatment with SRT2183 in Ly3 cells appears to be much less evident than the effects observed in Reh cells or Nalm-6 cells, suggesting a cell-specific effect under these conditions.

To demonstrate whether the response to SIRT1 activator alone or in combination with panobinostat is mediated by the upregulation of GADD45G, we performed experiments in cells transfected with GADD45G siRNA. Figure 6d shows that downregulation of GADD45G protects Reh cells from apoptotic effects in response to SRT2183 alone and in combination with panobinostat. These experiments demonstrate that GADD45G is a specific mediator of the response to this combination.

**SIRT1 activators-mediated GADD45G upregulation is associated with repression of NF- $\kappa$ B/STAT3 complex binding to its promoter.** It is established that c-Myc suppresses GADD45 gene expression.<sup>33,34</sup> Moreover, the TNF- $\kappa$ B signaling pathway differentially affects the expression of GADD45 family members, upregulating GADD45B and downregulating GADD45A and GADD45G at least partially through c-Myc expression.<sup>35</sup> Although it has been demonstrated that c-Myc regulates GADD45 directly,<sup>36,37</sup> there is no evidence that NF- $\kappa$ B regulates GADD45 at the promoter level. Furthermore, in our previous report we demonstrated that panobinostat-induced reactivation of GADD45G is associated with GADD45G promoter acetylation of H3 and H4.<sup>21</sup> Considering this evidence, to explain the synergistic upregulation of GADD45G in response to the combined treatment of panobinostat and SRT2183, we hypothesize that NF- $\kappa$ B may be a direct repressor of GADD45G and that the deacetylation of NF- $\kappa$ B mediated by SIRT1 activator may suppress NF- $\kappa$ B function as GADD45G repressor. Therefore, while on the one side the HDAC inhibitor panobinostat functions at the histone level, acetylating and consequently activating the GADD45G promoter, on the other side the SIRT1 activator may function



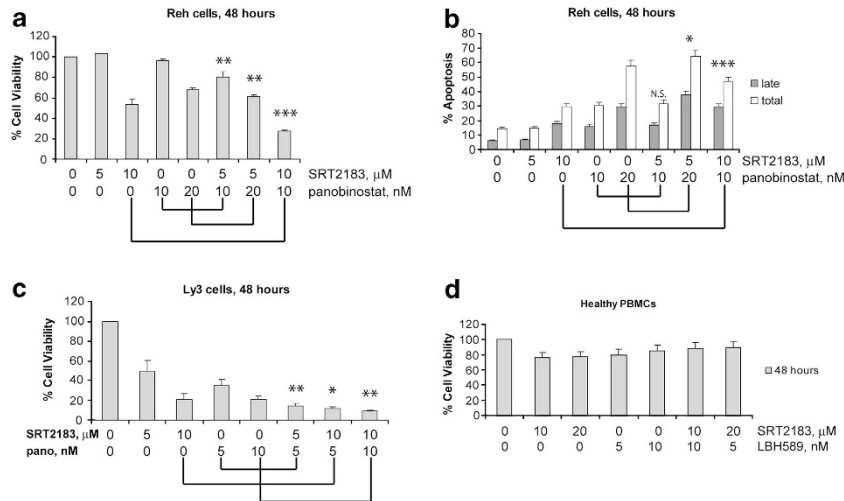


**Figure 4** Combination of SRT2183 with panobinostat induces more apoptosis than either compound alone in Reh cells. **(a)** Reh cells were treated for 48 h with the indicated concentrations of SRT2183, panobinostat, or a combination of these drugs. Following this, the percentage of cell viability was determined by MTS assay. Values represented as graphs are the mean of three independent experiments with S.D. **(b)** Reh cells were treated for 48 h with the indicated concentrations of SRT2183, panobinostat, or a combination of these drugs. Following this, the percentage of late apoptotic cells or total (early plus late) apoptosis was determined by flow cytometry using Annexin V/propidium iodide staining. Values represented as bar graphs are the mean of three independent experiments with the S.D. **(c)** Ly3 cells were treated for 48 h with the indicated concentrations of SRT2183, panobinostat, or a combination of these drugs. Following this, the percentage of cell viability was determined by MTS assay. Values represented as graphs are the mean of three independent experiments with S.D. **(d)** Peripheral blood mononuclear cells from a healthy donor were treated in culture for 48 h with the indicated concentrations of SRT2183, panobinostat, or a combination of these drugs. The percentage of viable cells was determined by DIMSCAN analysis. Values represent the percentages of cell viability normalized to that of the untreated cells and are the mean of three separate treatments. Statistical significance is relative to the single agent treatment inducing higher effect. NS, not significant, \* $P < 0.05$ , \*\* $P < 0.01$ , \*\*\* $P < 0.001$

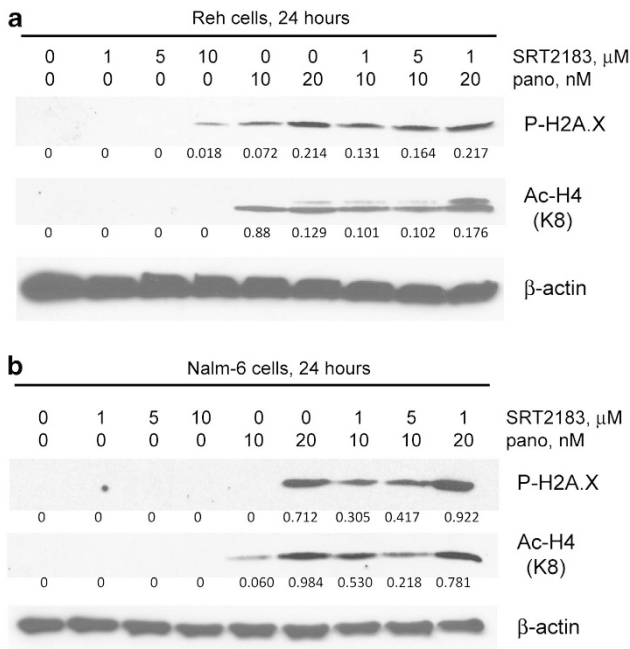


**Figure 5** Combination of SRT2183 with panobinostat induces greater phosphorylation of H2A.X and acetylation of H4 in ALL cell lines. **(a)** Reh cells and **(b)** NALM-6 cells were treated for 24 h with the indicated concentrations of SRT2183, panobinostat, or a combination of these drugs. Following this, western blot analysis of phospho-H2A.X and acetyl-H4 proteins was performed on the lysates from those cells. The levels of  $\beta$ -actin protein served as loading controls. Results are representative of three independent experiments

at the transcription factor level, deacetylating and consequently inhibiting the function of the GADD45G repressor. To test our hypothesis, we first performed chromatin

immunoprecipitation (ChIP) to determine the effects of SRT2183 on the DNA-binding levels of acetylated NF- $\kappa$ B and STAT3 at the GADD45G promoter in Ly3 and Reh cells. Figure 7a shows that SRT2183 treatment results in decreased levels of acetylated NF- $\kappa$ B and STAT3 bound to the GADD45G promoter in both the cell lines tested.

To determine whether the binding of NF- $\kappa$ B and STAT3 at the GADD45G promoter is direct or indirect, we first looked for potential NF- $\kappa$ B or STAT3 consensus binding sites in the first 2000 bases upstream the first ATG codon in the GADD45G gene. We found two NF- $\kappa$ B consensus binding sequences, at positions -1447 to -1438 (CBS G1) and -716 to -707 (CBS G3) relative to the translational start site. Based on these sequences, we designed two oligos for electrophoretic mobility shift assays (EMSA), oligo no. G1 and oligo no. G3, respectively, together with an oligo (oligo no. G2) containing a non-perfect NF- $\kappa$ B consensus sequence in the GADD45G gene (position -936 to -927, CBS G2) and a positive control oligo (oligo no. C1), which has been modified from a previously described oligo.<sup>38</sup> Oligo sequences are depicted in the Materials and Methods section. The map of the GADD45G promoter with the primers for ChIP assay and the oligos for EMSA are shown in Supplementary Figure S4. We also found nine non-perfect STAT3 consensus binding sequences in the same region at the GADD45G promoter. Figure 7b shows the results of a competition EMSA performed with both control and Ly3 cell nuclear extracts using the four unlabeled ('cold') oligos mentioned above plus a cold NF- $\kappa$ B control oligo (oligo no. C2), in combination with NF- $\kappa$ B-32P control oligo no. C2, indicating that oligos nos. G1 and G3 are potentially binding consensus sequences for NF- $\kappa$ B at the GADD45G promoter. Competition EMSA was also performed with the nine cold oligos for potential STAT3 binding plus STAT3-32P

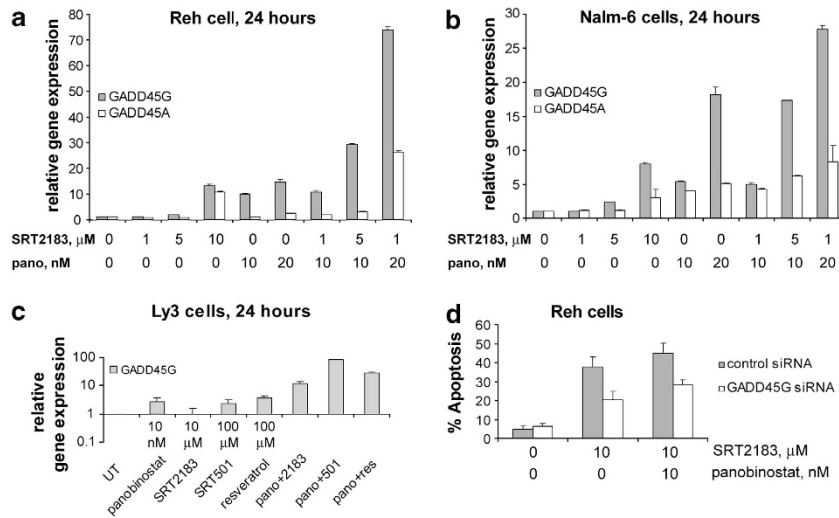


**Figure 6** Combination of SIRT2183 with panobinostat induces greater upregulation of GADD45G and GADD45A genes than either compound alone in pre-B ALL cell lines. (a) Reh cells, (b) NALM-6 cells and (c) Ly3 cells were treated for 24 h with the indicated concentrations of panobinostat and SIRT1 activators as single agents or in combination with panobinostat. Following this, TaqMan real-time PCR was performed. The mRNA levels were normalized to levels of  $\beta$ -actin mRNA. Values represented as bar graphs are the mean of three independent experiments with S.D. Data are expressed as  $2^{\Delta\Delta Ct}$ . (d) Reh cells were transfected with Cy3-labeled GADD45G siRNA or negative control siRNA and treated, 48 h later, with the indicated concentrations of SIRT2183, panobinostat, or a combination of these drugs. At 48 h after treatment, the percentage of apoptotic cells was determined in the gated Cy3-positive cell population, by flow cytometry using Annexin V/DAPI staining. Values represented as bar graphs are the mean of three independent experiments with S.D.

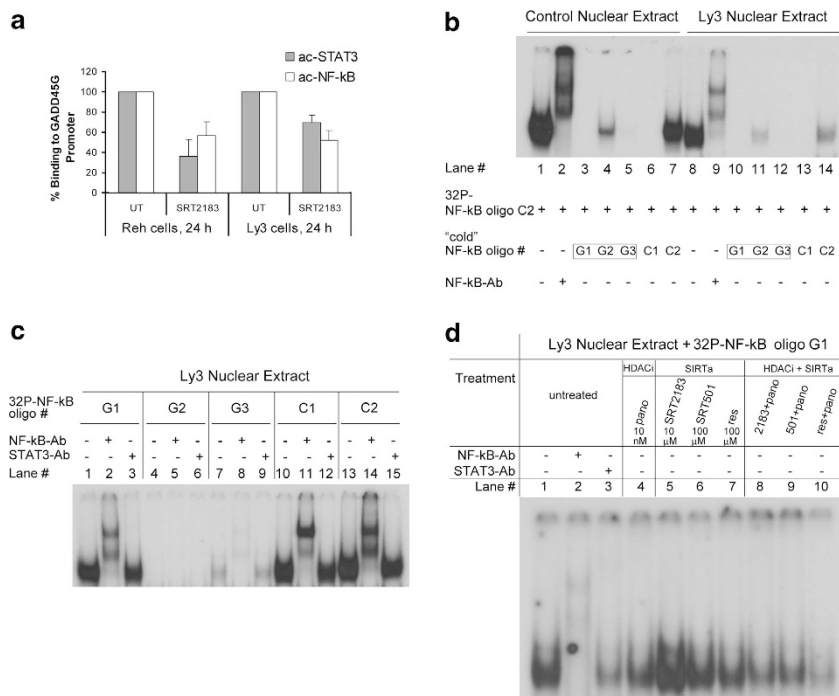


**Figure 7** Effects of SIRT1 activators alone or in combination with panobinostat on the binding of NF- $\kappa$ B and STAT3 to the GADD45G promoter. (a) Following treatment with 10  $\mu$ M SIRT2183 for 24 h, ChIP assay was performed on Reh and Ly3 cells. DNAs purified from the sheared cross-linked chromatin immunoprecipitated with anti-acetyl-STAT3 or anti-acetyl-NF- $\kappa$ B antibodies were used as TaqMan real-time PCR templates to amplify the GADD45G promoter region from -567 to +6. Inputs were used to normalize. Values represented as bar graphs are the mean of three independent experiments with S.D. (b) Competition EMSA: Effect of unlabeled ('cold') oligonucleotides G1, G2, and G3 on NF- $\kappa$ B DNA-binding activity. Lanes 1–7: Nuclear extract from lipopolysaccharide LPS-stimulated macrophages. Lanes 8–14: Nuclear extract from Ly3 cells. 'Cold' oligonucleotides G1–G3 and C1 were added in 100-fold molar excess. C2 was added 1 : 1, as compared with control 32P-labeled NF- $\kappa$ B oligo C2. Lanes 2 and 9 contain NF- $\kappa$ B antibodies (supershift). (c) DNA-binding activity (EMSA assay) of NF- $\kappa$ B to 32P-labeled NF- $\kappa$ B consensus sequences G1–G3 (lanes 1–9). Lanes 10–15: Control NF- $\kappa$ B oligonucleotides. Lanes 1–15: Nuclear extract from Ly3 cells. NF- $\kappa$ B and STAT3 antibodies were used in supershifts (lanes 2, 5, 8, 11, 14 and lanes 3, 6, 9, 12, 15, respectively). (d) Effect of compound-treated Ly3 cells on NF- $\kappa$ B DNA-binding activity (EMSA assay). Ly3 cells were treated with HDACi, SIRTa or HDACi + SIRTa as indicated. Nuclear extract of untreated (lanes 1–3) and treated cells (lanes 4–10) was isolated 24 h post treatment and incubated with 32P-labeled NF- $\kappa$ B oligonucleotide G1 before EMSA analysis. NF- $\kappa$ B and STAT3 antibodies were used in supershift (lanes 2 and 3, respectively)

control oligo, resulting in no potential binding of STAT3 to any of these oligo sequences (data not shown). EMSA results shown in Figure 7c not only demonstrate that NF- $\kappa$ B binds to oligos nos.G1 and G3 in Ly3 cell nuclear extracts but also that STAT3 may be in complex with NF- $\kappa$ B at the GADD45G promoter.

We then performed EMSA to evaluate the effect of SIRT1 activators alone or in combination with panobinostat on the binding of NF- $\kappa$ B to the GADD45G promoter. Figure 7d shows that SRT2183 (lane 5) does not reduce the DNA-binding capacity of NF- $\kappa$ B to the GADD45G promoter, while SRT501 (lane 6), resveratrol (lane 7), and panobinostat (lane 4) all decrease NF- $\kappa$ B-binding levels. Notably, the combination of panobinostat with all the three SIRT1 activators (lane 8–10) results in higher repression of NF- $\kappa$ B binding to the GADD45G promoter. Therefore, we wanted to determine whether the repression of NF- $\kappa$ B/STAT3 complex binding to the GADD45G promoter observed in Ly3 cells under those conditions correlates with the acetylation status of both the transcription factors. Figure 8a demonstrates that SIRT1 activators induce deacetylation of both NF- $\kappa$ B and STAT3, and decrease the acetyl-lysine levels in Ly3 cells. However, the combination of any of the SIRT1 activators with panobinostat recovers the acetylation level of NF- $\kappa$ B and lysine but still remains at lower level than those of the untreated or panobinostat-treated cells. Similar results were obtained for STAT3.

## Discussion

In the present study, we investigated the activity of two SIRT1 activators, SRT501 and SRT2183, in a panel of malignant lymphoid cell lines. Cells were treated with either SRT501 or SRT2183, as well as in combination with panobinostat, and evaluated for biological and gene expression responses. Due to contrasting observations, it is still controversial whether SIRT1 activation or its inhibition has more anti-tumor activity. Our results demonstrate that activation of SIRT1 leads to anti-tumor responses in the cells studied here. Both SRT501 and SRT2183 induced growth arrest and apoptosis, with SRT2183 more potent than SRT501. These biological effects were associated with deacetylation of STAT3 and NF- $\kappa$ B p65 proteins, consistent with previous evidence of the inhibitory effect of resveratrol on both signaling pathways.<sup>10–15</sup> We also observed a reduction of the protein levels of c-Myc, which is a target of both STAT3 and NF- $\kappa$ B,<sup>31</sup> and this correlates with the decreased level of cell proliferation.

PCR array analysis revealed that SRT2183 treatment leads to increased mRNA levels of pro-apoptosis, growth arrest, and DNA-damage-response genes. Interestingly, one of the genes whose expression levels were the most increased is GADD45G, which was the most dramatically upregulated gene in ALL cell lines following panobinostat treatment.<sup>21</sup> It has been shown that in response to oxidative stress or nitric oxide SIRT1 increases transactivation activity of FOXO4 or FOXO1, which consequently induces GADD45A expression.<sup>39,40</sup> Moreover, resveratrol and its analogs induce the expression of p53-responsive genes, such as GADD45A.<sup>41–43</sup> Our findings represent the first evidence that associates SIRT1 activation with GADD45G upregulation. Gene expression

changes were accompanied by accumulation of phospho-H2A.X levels, which is one of the earliest responses to DNA damage.<sup>32</sup> Combination of SRT2183 with HDAC inhibitor panobinostat enhanced the anti-proliferative and anti-survival effects mediated by either compounds alone. The combination of panobinostat plus SRT2183 also showed greater inhibition of c-Myc protein levels and phosphorylation of H2A.X. Interestingly, this combination also increased acetylation of H4 and of p53. Quantitative real-time PCR confirmed that the combination of panobinostat with SRT2183 leads to significantly higher expression of GADD45G than either agent alone. This upregulation of GADD45G expression was also observed in the combination of panobinostat with either SRT501 or resveratrol.

Importantly, our siRNA experiments demonstrate that the response to SIRT1 activator alone or in combination with panobinostat is mediated by the upregulation of GADD45G. We have previously demonstrated, by siRNA experiments, that GADD45G upregulation mediates the response to panobinostat treatment in pre-B- and T-leukemic cells,<sup>21</sup> and that this upregulation is associated with histone hyperacetylation at the gene promoter level.<sup>21</sup> Here we demonstrate in addition that GADD45G siRNA rescues Reh cells from apoptosis induced by SRT2183 alone or in combination with panobinostat. Although we provide evidence that GADD45G is a specific mediator of the response to this combination, we do not exclude the possibility that other genes also may be involved in the response.

Here we hypothesized that a SIRT1 activator may upregulate GADD45G by inhibiting its potential corepressors at the transcriptional level. ChIP assays revealed that both acetylated NF- $\kappa$ B and STAT3 are bound to the GADD45G promoter and that SRT2183 decreases these levels, suggesting that the DNA-binding capacity of both NF- $\kappa$ B and STAT3 at the promoter of GADD45G is inhibited by the SIRT1 activator. Furthermore, EMSA revealed that NF- $\kappa$ B binds directly to GADD45G promoter, while STAT3 binds indirectly via complexes with NF- $\kappa$ B. EMSA also demonstrated that binding of this NF- $\kappa$ B/STAT3 complex to the GADD45G promoter is inhibited following panobinostat, SRT501, or resveratrol treatment and that the combination of panobinostat with SRT2183, SRT501 or resveratrol induces a greater binding repression than either agent alone.

NF- $\kappa$ B is a negative regulator of GADD45G via c-Myc.<sup>44</sup> This is the first report showing direct binding of NF- $\kappa$ B to the promoter of GADD45G. Although there is evidence suggesting that the expression of OIG37 (murine GADD45g) is regulated by the STAT3 pathway,<sup>45</sup> it is not known yet whether STAT3 directly regulates the expression of human GADD45 gene family members. This is the first study demonstrating that STAT3 binds indirectly to the GADD45G promoter in complexes with NF- $\kappa$ B, which in turn binds directly, suggesting for the first time that STAT3 regulates GADD45G at the transcriptional level as a corepressor with NF- $\kappa$ B of a GADD45 family member.

NF- $\kappa$ B p65 and STAT3 are typically associated with transcriptional activation. However, Lee *et al.*<sup>46</sup> demonstrated that STAT3 can also function as repressor. They demonstrated that acetylated STAT3 function as a transcriptional repressor by inducing hypermethylation of certain gene

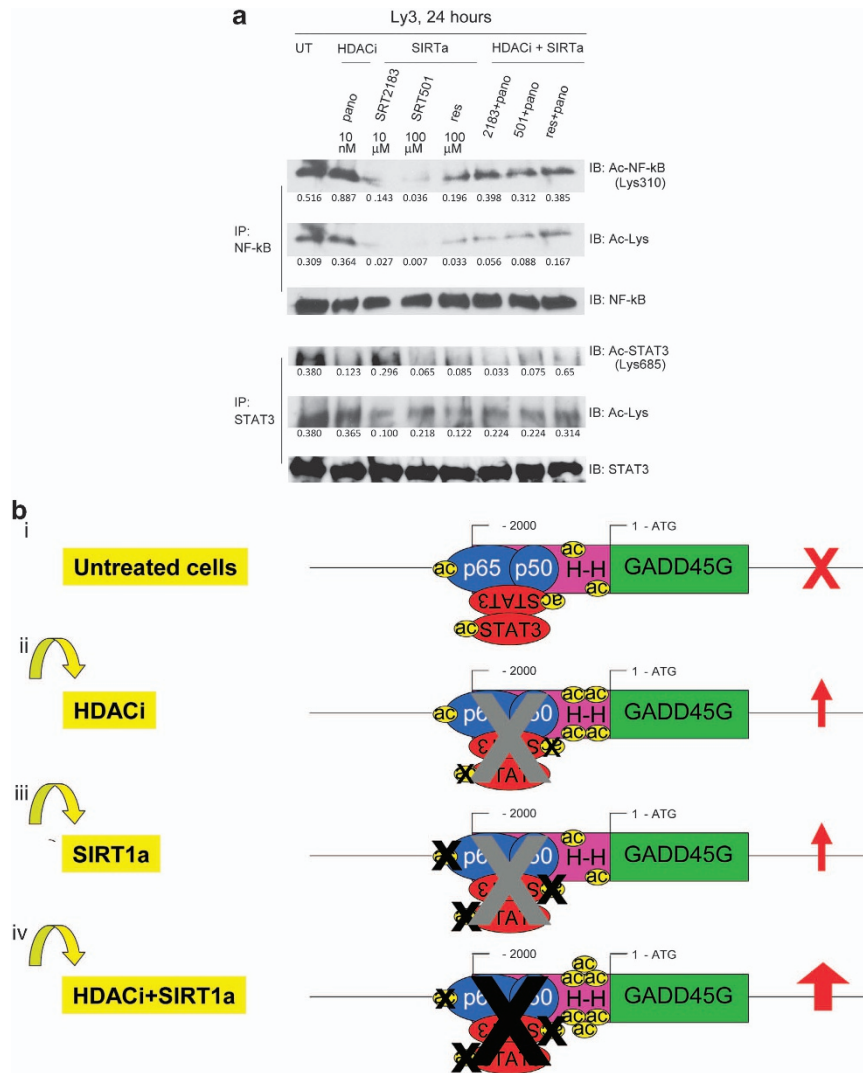


**Figure 8** A model to explain the greater upregulation of GADD45G mediated by the combination of a SIRT1 activator with a class I, II, and IV HDAC inhibitor. (a) Ly3 cells were treated with the indicated concentrations of panobinostat, and SIRT1 activators as single agents or in combination with panobinostat for 24 h. Following this, immunoprecipitation (IP) and subsequent immunoblotting (IB) were performed on the cell lysates to analyze acetyl-STAT3 and acetyl-NF-κB levels. The levels of total STAT3 and total NF-κB served as loading controls. (b) Predicted acetylation status of histones and STAT3/NF-κB complexes at the GADD45G promoter in untreated cells (i) and in cells treated with an HDACi (ii), a SIRT1a (iii), and the combination of an HDACi with a SIRT1a (iv)

promoters. There is also evidence of NF-κB p65 functioning as a transcriptional repressor. Liu *et al.*<sup>47</sup> demonstrated that NF-κB p65 can also function as a transcriptional repressor through enhanced methylation of a certain gene promoter. Our data demonstrate a correlation between inhibition of the binding of acetylated NF-κB p65 and STAT3 at the GADD45G promoter in response to treatment with a SIRT1 activator and upregulation of the GADD45G gene. Therefore, we speculate that in this context STAT3 and NF-κB p65 may function as a GADD45G repressor complex at the promoter level, perhaps by inducing chromatin modification. Thus, these data suggest that the upregulation of GADD45G may be due to the inhibition of its repressors by SIRT1 activators.

Taking all these data together, we propose a model explaining the mechanism of action of a SIRT1 activator *versus* a class I, II, and IV HDAC inhibitor either alone or in combination (Figure 8b). Importantly, GADD45G is frequently

inactivated epigenetically in multiple tumors.<sup>48</sup> Previously, we demonstrated that GADD45G silencing is associated to low histone acetylation at the promoter level. Here we demonstrate that in untreated tumor cells, STAT3 and NF-κB are in complexes as corepressors at the GADD45G promoter and both are acetylated in these complexes (Figure 8bi). When cells are treated with panobinostat, GADD45G is reactivated, associated with hyperacetylation of the histones at the promoter level, as we previously demonstrated. Panobinostat does not induce greater acetylation of the corepressors but instead leads to decreased binding of the corepressors to the GADD45G promoter, suggesting that either the acetylation of the histones at the promoter may destabilize the anchoring of the corepressor complexes or the corepressor complexes may sense the acetylation of the promoter as a reactivation signal for GADD45G (Figure 8bii). When cells are treated with the SIRT1 activator, GADD45G is reactivated, associated



with decreased binding of the corepressors to the GADD45G promoter and correlating with the deacetylation of both STAT3 and NF- $\kappa$ B (Figure 8biii). By contrast, when cells are treated with the combination of panobinostat with a SIRT1 activator, GADD45G is synergistically reactivated, associated with greater acetylation of H3 and H4. Moreover, panobinostat, in the combination treatment, recovers partially the acetylation status of NF- $\kappa$ B; nevertheless, the combination leads to greater inhibition binding of the corepressors to the GADD45G promoter (Figure 8biv).

In sum, our observations suggest that it is either the balance of the acetylation of histones and corepressors or the crosstalk between them, that results in the reactivation of GADD45G and the biological outcome. Moreover, the SIRT1 activators SRT501 and SRT2183 show growth inhibitory and pro-apoptotic activity in malignant lymphoid cells alone as well as further enhanced activity in combination with panobinostat. At least one of the mechanisms of action, which explains the combination effect, is mediated through enhanced upregulation of GADD45G as a result of the repressed binding of NF- $\kappa$ B/STAT3 complexes to the GADD45G promoter together with hyperacetylation of this promoter. Given the known broad spectrum activity of these agents, we do not exclude the possibility that mechanisms other than STAT3/NF- $\kappa$ B inhibition and GADD45G reactivation may be involved in the response to SIRT1 activator alone or in combination to panobinostat. Nevertheless, we propose that this is an important component of the growth inhibitory and pro-apoptotic activity of SIRT1 activators. Thus, our study not only associates SIRT1 activation with GADD45G upregulation and demonstrates for the first time STAT3 as a corepressor with NF- $\kappa$ B of GADD45G but also provide *in vitro* proof-of-concept that the combination of class I, II, and IV HDAC inhibitors with SIRT1 activators may be a potential new therapeutic strategy for lymphoid malignancies.

## Materials and Methods

**Drugs.** SIRT1 activators SRT501 and SRT2183 were provided by Sirtris (Cambridge, MA, USA), SIRT1 activator resveratrol was purchased from Sigma (St. Louis, MO, USA). HDAC inhibitor panobinostat was provided by Novartis (Cambridge, MA, USA). For *in vitro* experiments, all drugs except for resveratrol were dissolved in 100% dimethyl sulfoxide (DMSO) to prepare 8 mM (SRT2183), 40 mM (SRT501), and 5 mM (panobinostat) stocks and stored at  $-80^{\circ}\text{C}$ . Resveratrol was dissolved in absolute ethanol to prepare a 50 mM stock and stored at  $-20^{\circ}\text{C}$ . The final DMSO concentration used in all the treatment conditions was not higher than 0.25%. Supplementary Figures S1A–C demonstrates that the results obtained from the treated cells reflect the effects of the SRT compounds and not of DMSO.

**Cell lines and cell culture conditions.** Human Philadelphia chromosome-negative ALL Reh (pre-B cells), NALM-6 (pre-B cells) and MOLT-4 (T cells), Burkitt's lymphoma Daudi and Raji, and multiple myeloma U266 cell lines were obtained from American Type Culture Collection (Manassas, VA, USA). Human Hodgkin's lymphoma L450, ABC-like DLBCL DHL-8 and mantle cell lymphoma REC-1 cell lines were obtained from DSMZ (Deutsche Sammlung von Mikroorganismen und Zellkulturen GmbH; Braunschweig, Germany). Human ABC-like DLBCL Ly3, germinal center-like DLBCL DHL-6, and Burkitt's lymphoma 2F7 cell lines were a gift from Drs. B. Hilda Ye (Albert Einstein College of Medicine, Bronx, NY, USA), M. Jensen (Seattle Children's Research Institute, Seattle, WA, USA) and O. Martinez-Maza (David Geffen School of Medicine, UCLA, USA), respectively. All cells were maintained in RPMI-1640 medium (Iscove's Modified Dulbecco's medium for Ly3 cells) containing 10% fetal bovine serum and 50 units/ml penicillin and streptomycin at  $37^{\circ}\text{C}$  in an atmosphere of 5%  $\text{CO}_2$  and passaged twice a week.

**Cell viability analysis by MTS assays.** Cells were seeded in 96-well plates at a density of 10 000 cells/well. After 24, 48, or 72 h, cell viability was determined by assaying with MTS assay (Promega, Madison, WI, USA). The MTS assay was performed according to instructions from the supplier. Absorbance was measured at 490 nm with a Chameleon plate reader (Bioscan, Washington DC, USA).

**Apoptosis analysis by flow cytometry.** Untreated and drug-treated cells were stained with Annexin V and propidium iodide (PI) using Annexin V-fluorescein isothiocyanate Apoptosis Detection Kit I (BD Biosciences Pharmingen, San Diego, CA, USA). The percentage of apoptotic cells was determined by flow cytometry. At least 50 000 cells were collected with a CyAn ADP Violet (Beckman Coulter, Miami, FL, USA) cytometer and calculated using the software Summit 4.3 (Beckman Coulter). Percentage of apoptosis in Figures 2a and b was calculated based on all the Annexin V-positive (early apoptotic) plus the Annexin V/PI-positive (late apoptotic) cells.

**PCR arrays and quantitative real-time PCR.** Total RNA was isolated and purified from cells by RNeasy Kit (Qiagen, Valencia, CA, USA) and reverse-transcribed using the Omniscript Reverse Transcription Kit (Qiagen). For Supplementary Table S1, complementary deoxyribonucleic acids (cDNAs) were analyzed using a PCR array system (SABiosciences, Valencia, CA, USA) according to the manufacturer's protocol. For Figures 6a, b, c and 7a, cDNAs were analyzed by quantitative real-time PCR (qRT-PCR) using primers previously described<sup>21</sup> and iQ SYBR Green supermix (Bio-Rad Laboratories, Hercules, CA, USA). PCRs were carried out on a DNA Engine thermal cycler equipped with Chromo4 detector (Bio-Rad).

**Protein immunoprecipitation.** Cell lysates (250  $\mu\text{g}$  protein) were incubated with NF- $\kappa$ B or STAT3 antibodies (Cell Signaling Technology, Danvers, MA, USA) overnight at  $4^{\circ}\text{C}$ . To this mixture, washed protein A beads were added and incubated for 1 h at  $4^{\circ}\text{C}$ . Next, the immunoprecipitates were washed five times with the lysis buffer and proteins were eluted with the sodium dodecyl sulfate (SDS) sample buffer, loaded on SDS polyacrylamide gel electrophoresis (SDS-PAGE) gels and analyzed by western blotting analysis using ac-NF- $\kappa$ B, ac-STAT3, or ac-Lys antibodies (Cell Signaling Technology).

**Western blot analysis.** Cells were washed with ice-cold phosphate-buffered saline containing 0.1 mM sodium orthovanadate and total proteins were isolated using radioimmunoprecipitation lysis buffer lysis buffer, which included protease inhibitors (leupeptin, antipain, and aprotinin), 0.5 mM phenylmethanesulfonyl fluoride and 0.2 mM sodium orthovanadate. Protein amounts were quantified using the Bio-Rad protein assay (Bio-Rad). Equal amounts of proteins were loaded onto a SDS-PAGE gel, transferred onto nitrocellulose membrane, and probed with the indicated antibody: rabbit anti-acetyl-STAT3 (Lys685), rabbit anti-phospho-STAT3 (Tyr705), rabbit anti-acetyl-NF- $\kappa$ B p65 (Lys310), rabbit anti-phospho-NF- $\kappa$ B p65 (Ser536), rabbit anti-phospho-H2A.X (Ser139), rabbit anti-acetyl-H4 (Lys8), rabbit anti-acetyl-p53 (Lys382) (Cell Signaling Technology); mouse anti-c-Myc (Santa Cruz Biotechnology, Santa Cruz, CA, USA); and mouse  $\beta$ -actin antibody (Sigma-Aldrich, St. Louis, MO, USA). Membranes were then washed, reprobed with appropriate horseradish peroxidase-conjugated secondary antibodies (Amersham Biosciences, Buckinghamshire, UK), and developed with SuperSignal chemiluminescent substrate (Pierce Biotechnology, Rockford, IL, USA).

**ChIP.** ChIP analysis was conducted as described by EZ-ChIP Chromatin Immunoprecipitation Kit from Upstate Biotechnologies (Temecula, CA, USA). The chromatin was immunoprecipitated with normal rabbit IgG, anti-acetyl-STAT3 (Lys685; Cell Signaling Technology), and anti-acetyl-NF- $\kappa$ B p65 (Lys310; Abcam, Cambridge, MA, USA) antibodies. Ten percent of the supernatant fraction from the sheared cross-linked chromatin lacking primary antibody was saved as the 'input.' DNAs were purified and used as the real-time PCR templates to amplify the TGADD45GT promoter regions from  $-567$  to  $+6$  relative to the translation initiation site. The sequences of the primers were as follows: forward: 5'-TCTGGCTCCAATGCAACAGTCTCA-3'; and reverse: 5'-AGTCATAGTGCAGTCAACACAGCAG-3'.

**Nuclear extract preparation and EMSA.** To detect DNA-binding activity of NF- $\kappa$ B and STAT3 by EMSA, nuclear protein extracts were prepared using high-salt extraction as previously described.<sup>49</sup> Nuclear proteins (5  $\mu\text{g}$ ) from Ly3

cells or lipopolysaccharide-stimulated macrophages (source of activated NF- $\kappa$ B, control nuclear extract) were incubated at 37 °C for 30 min with the following 32P- or non-radioactive ('cold') double-stranded oligonucleotides:

- Oligo G1 (– 1447 to – 1438): 5'-AGCTTGATGGGAATTCCTTTTG-3';  
Oligo G2 (– 936 to – 927): 5'-AGCTGCGGCGGGTCTGCCACC-3';  
Oligo G3 (– 716 to – 707): 5'-AGCTGGGTGGGATCTCCAGAGA-3';  
Oligo C1 (positive control): 5'-AGCTATTAGGGGATGCCCTCATG-3' and  
Oligo C2 (positive control): 5'-TCGACAGAGGGGACTTCCGAG-3'.

NF- $\kappa$ B antibody (mixture of p50 SC-114X, p65 SC-372X, and c-Rel SC-70X antibodies, Santa Cruz Biotechnology) and STAT3 antibody (C20X, Santa Cruz Biotechnology) were used to identify NF- $\kappa$ B and STAT3 in 'super-shift' assays. For super-shift assays, concentrated antibody (3  $\mu$ l) was preincubated with nuclear proteins 20 min before the addition of radiolabeled/cold probe and separation by nondenaturing PAGE and autoradiographic detection.

**siRNA design and transfection.** The Cy3-labeled GADD45G siRNA was designed and synthesized as previously described.<sup>21</sup> The Cy3-labeled negative control siRNA was obtained from IDT (Coralville, IA, USA). Transient transfections of Reh cells were performed with the Nucleofector Kit L, program L-29 (Amaxa Biosystems, Gaithersburg, MD, USA). Five hundred nanomolar siRNA was used in each transfection with two million cells.

**Statistical analysis and software.** The data shown represent mean values of at least three independent experiments and expressed as mean  $\pm$  S.D. Statistical analyses were performed by the Student's *t*-test, using the statistical software GraphPad Prism 4 (GraphPad Software, San Diego, CA, USA). Statistical significance was set at a level of  $P < 0.05$ . The integrated density value values were normalized to those of  $\beta$ -actin or total proteins, which were determined by the densitometry software Alphamager (ProteinSimple, Santa Clara, CA, USA). The IC<sub>50</sub> values in Figure 1c and the CI values were calculated by the software Compusyn (ComboSyn, Paramus, NJ, USA); the descriptions of the effect in the combinations are based on the ranges of CI refined from those described by Chou.<sup>50</sup>

### Conflict of Interest

JMC is employed by and has declared a financial interest in Sirtris Pharmaceuticals, whose products, SRT2183 and SRT501, were studied in the present work. PA is employed by and has declared a financial interest in Novartis Pharmaceuticals, whose product, panobinostat, was studied in the present work. The other authors declare no conflict of interest.

**Acknowledgements.** This work was supported by a grant from the National Institute of Health (R01 CA-055652) to RJ, W. M. Keck Foundation and Tim Nesvig Lymphoma Fellowships to AS. We thank members of our laboratories for stimulating discussion and the Analytical Cytometry Core at the City of Hope.

- Stimson L, Wood V, Khan O, Fotheringham S, La Thangue NB. HDAC inhibitor-based therapies and haematological malignancy. *Ann Oncol* 2009; **20**: 1293–1302.
- Piekarz RL, Frye R, Turner M, Wright JJ, Allen SL, Kirschbaum MH et al. Phase II multi-institutional trial of the histone deacetylase inhibitor romidepsin as monotherapy for patients with cutaneous T-cell lymphoma. *J Clin Oncol* 2009; **27**: 5410–5417.
- Kirschbaum M, Frankel P, Popplewell L, Zain J, Delioukina M, Pullarkat V et al. Phase II study of vorinostat for treatment of relapsed or refractory indolent non-Hodgkin's lymphoma and mantle cell lymphoma. *J Clin Oncol* 2011; **29**: 1198–1203.
- Frye RA. Characterization of five human cDNAs with homology to the yeast SIR2 gene: Sir2-like proteins (sirtuins) metabolize NAD and may have protein ADP-ribosyltransferase activity. *Biochem Biophys Res Commun* 1999; **260**: 273–279.
- Finkel T, Deng CX, Mostoslavsky R. Recent progress in the biology and physiology of sirtuins. *Nature* 2009; **460**: 587–591.
- Bosch-Presegue L, Vaquero A. The dual role of sirtuins in cancer. *Genes Cancer* 2011; **2**: 648–662.
- Blum CA, Ellis JL, Loh C, Ng PY, Perni RB, Stein RL. SIRT1 modulation as a novel approach to the treatment of diseases of aging. *J Med Chem* 2011; **54**: 417–432.
- Pruitt K, Zinn RL, Ohm JE, McGarvey KM, Kang SH, Watkins DN et al. Inhibition of SIRT1 reactivates silenced cancer genes without loss of promoter DNA hypermethylation. *PLoS Genet* 2006; **2**: e40.
- Audrito V, Vaisitti T, Rossi D, Gottardi D, D'Arena G, Laurenti L et al. Nicotinamide blocks proliferation and induces apoptosis of chronic lymphocytic leukemia cells through activation of the p53/miR-34a/SIRT1 tumor suppressor network. *Cancer Res* 2011; **71**: 4473–4483.
- Singh NP, Singh UP, Hegde VL, Guan H, Hofseth L, Nagarkatti M et al. Resveratrol (trans-3,5,4'-trihydroxystilbene) suppresses EL4 tumor growth by induction of apoptosis involving reciprocal regulation of SIRT1 and NF-kappaB. *Mol Nutr Food Res* 2011; **55**: 1207–1218.
- Bhardwaj A, Sethi G, Vadhan-Raj S, Bueso-Ramos C, Takada Y, Gaur U et al. Resveratrol inhibits proliferation, induces apoptosis, and overcomes chemoresistance through down-regulation of STAT3 and nuclear factor-kappaB-regulated antiapoptotic and cell survival gene products in human multiple myeloma cells. *Blood* 2007; **109**: 2293–2302.
- Sun C, Hu Y, Liu X, Wu T, Wang Y, He W et al. Resveratrol downregulates the constitutive activation of nuclear factor-kappaB in multiple myeloma cells, leading to suppression of proliferation and invasion, arrest of cell cycle, and induction of apoptosis. *Cancer Genet Cytogenet* 2006; **165**: 9–19.
- Li T, Wang W, Chen H, Li T, Ye L. Evaluation of anti-leukemia effect of resveratrol by modulating STAT3 signaling. *Int Immunopharmacol* 2010; **10**: 18–25.
- Estrov Z, Shishodia S, Faderl S, Harris D, Van Q, Kantarjian HM et al. Resveratrol blocks interleukin-1beta-induced activation of the nuclear transcription factor NF-kappaB, inhibits proliferation, causes S-phase arrest, and induces apoptosis of acute myeloid leukemia cells. *Blood* 2003; **102**: 987–995.
- Asou H, Koshizuka K, Kyo T, Takata N, Kamada N, Koefler HP. Resveratrol, a natural product derived from grapes, is a new inducer of differentiation in human myeloid leukemias. *Int J Hematol* 2002; **75**: 528–533.
- Smith JJ, Kenney RD, Gagne DJ, Frushour BP, Ladd W, Galonek HL et al. Small molecule activators of SIRT1 replicate signaling pathways triggered by calorie restriction in vivo. *BMC Syst Biol* 2009; **3**: 31.
- Howitz KT, Bitterman KJ, Cohen HY, Lamming DW, Lavu S, Wood JG et al. Small molecule activators of sirtuins extend *Saccharomyces cerevisiae* lifespan. *Nature* 2003; **425**: 191–196.
- Milne JC, Lambert PD, Schenk S, Carney DP, Smith JJ, Gagne DJ et al. Small molecule activators of SIRT1 as therapeutics for the treatment of type 2 diabetes. *Nature* 2007; **450**: 712–716.
- Dai H, Kustigian L, Carney D, Case A, Considine T, Hubbard BP et al. SIRT1 activation by small molecules: kinetic and biophysical evidence for direct interaction of enzyme and activator. *J Biol Chem* 2010; **285**: 32695–32703.
- Hubbard BP, Gomes AP, Dai H, Li J, Case AW, Considine T et al. Evidence for a common mechanism of SIRT1 regulation by allosteric activators. *Science* 2013; **339**: 1216–1219.
- Scuto A, Kirschbaum M, Kowolik C, Kretzner L, Juhasz A, Atadja P et al. The novel histone deacetylase inhibitor, LBH589, induces expression of DNA damage response genes and apoptosis in Ph- acute lymphoblastic leukemia cells. *Blood* 2008; **111**: 5093–5100.
- Nie Y, Erion DM, Yuan Z, Dietrich M, Shulman GI, Horvath TL et al. STAT3 inhibition of gluconeogenesis is downregulated by SirT1. *Nat Cell Biol* 2009; **11**: 492–500.
- Sestito R, Madonna S, Scarponi C, Cianfarani F, Failla CM, Cavani A et al. STAT3-dependent effects of IL-22 in human keratinocytes are counterregulated by sirtuin 1 through a direct inhibition of STAT3 acetylation. *FASEB J* 2011; **25**: 916–927.
- Bernier M, Paul RK, Martin-Montalvo A, Scheibye-Knudsen M, Song S, He HJ et al. Negative regulation of STAT3 protein-mediated cellular respiration by SIRT1 protein. *J Biol Chem* 2011; **286**: 19270–19279.
- Yeung F, Hoberg JE, Ramsey CS, Keller MD, Jones DR, Frye RA et al. Modulation of NF-kappaB-dependent transcription and cell survival by the SIRT1 deacetylase. *EMBO J* 2004; **23**: 2369–2380.
- Yuan ZL, Guan YJ, Chatterjee D, Chin YE. Stat3 dimerization regulated by reversible acetylation of a single lysine residue. *Science* 2005; **307**: 269–273.
- Chen LF, Mu Y, Greene WC. Acetylation of RelA at discrete sites regulates distinct nuclear functions of NF-kappaB. *EMBO J* 2002; **21**: 6539–6548.
- Lam LT, Wright G, Davis RE, Lenz G, Farinha P, Dang L et al. Cooperative signaling through the signal transducer and activator of transcription 3 and nuclear factor-(kappa)B pathways in subtypes of diffuse large B-cell lymphoma. *Blood* 2008; **111**: 3701–3713.
- Chen LF, Williams SA, Mu Y, Nakano H, Duerr JM, Buckbinder L et al. NF-kappaB RelA phosphorylation regulates RelA acetylation. *Mol Cell Biol* 2005; **25**: 7966–7975.
- Kiuchi N, Nakajima K, Ichiba M, Fukada T, Narimatsu M, Mizuno K et al. STAT3 is required for the gp130-mediated full activation of the c-myc gene. *J Exp Med* 1999; **189**: 63–73.
- Han SS, Yun H, Son DJ, Tompkins VS, Peng L, Chung ST et al. NF-kappaB/STAT3/PI3K signaling crosstalk in iMyc E mu B lymphoma. *Mol Cancer* 2010; **9**: 97.
- Thiriet C, Hayes JJ. Chromatin in need of a fix: phosphorylation of H2AX connects chromatin to DNA repair. *Mol Cell* 2005; **18**: 617–622.
- Marhin WW, Chen S, Facchini LM, Fornace AJ Jr., Penn LZ. Myc represses the growth arrest gene gadd45. *Oncogene* 1997; **14**: 2825–2834.
- Bush A, Mateyak M, Dugan K, Obaya A, Adachi S, Sedivy J et al. c-myc null cells misregulate cad and gadd45 but not other proposed c-Myc targets. *Genes Dev* 1998; **12**: 3797–3802.
- Zerbini LF, Wang Y, Czibere A, Correa RG, Cho JY, Ijiri K et al. NF-kappa B-mediated repression of growth arrest- and DNA-damage-inducible proteins 45alpha and gamma is essential for cancer cell survival. *Proc Natl Acad Sci USA* 2004; **101**: 13618–13623.

36. Amundson SA, Zhan Q, Penn LZ, Fornace AJ Jr. Myc suppresses induction of the growth arrest genes gadd34, gadd45, and gadd153 by DNA-damaging agents. *Oncogene* 1998; **17**: 2149–2154.
37. Tao H, Umek RM. Reciprocal regulation of gadd45 by C/EBP alpha and c-Myc. *DNA Cell Biol* 1999; **18**: 75–84.
38. Lee H, Herrmann A, Deng JH, Kujawski M, Niu G, Li Z *et al*. Persistently activated Stat3 maintains constitutive NF-kappaB activity in tumors. *Cancer Cell* 2009; **15**: 283–293.
39. Kobayashi Y, Furukawa-Hibi Y, Chen C, Horio Y, Isobe K, Ikeda K *et al*. SIRT1 is critical regulator of FOXO-mediated transcription in response to oxidative stress. *Int J Mol Med* 2005; **16**: 237–243.
40. Hughes KJ, Meares GP, Hansen PA, Corbett JA. FoxO1 and SIRT1 regulate beta-cell responses to nitric oxide. *J Biol Chem* 2011; **286**: 8338–8348.
41. Zheng JP, Ju D, Jiang H, Shen J, Yang M, Li L. Resveratrol induces p53 and suppresses myocardin-mediated vascular smooth muscle cell differentiation. *Toxicol Lett* 2010; **199**: 115–122.
42. Li G, He S, Chang L, Lu H, Zhang H, Zhang H *et al*. GADD45alpha and annexin A1 are involved in the apoptosis of HL-60 induced by resveratrol. *Phytomedicine* 2011; **18**: 704–709.
43. Lu J, Ho CH, Ghai G, Chen KY. Resveratrol analog, 3,4,5,4'-tetrahydroxystilbene, differentially induces pro-apoptotic p53/Bax gene expression and inhibits the growth of transformed cells but not their normal counterparts. *Carcinogenesis* 2001; **22**: 321–328.
44. Zerbinì LF, Libermann TA. Life and death in cancer. GADD45 alpha and gamma are critical regulators of NF-kappaB mediated escape from programmed cell death. *Cell Cycle* 2005; **4**: 18–20.
45. Nakayama K, Hara T, Hibi M, Hirano T, Miyajima A. A novel oncostatin M-inducible gene OIG37 forms a gene family with MyD118 and GADD45 and negatively regulates cell growth. *J Biol Chem* 1999; **274**: 24766–24772.
46. Lee H, Zhang P, Herrmann A, Yang C, Xin H, Wang Z *et al*. Acetylated STAT3 is crucial for methylation of tumor-suppressor gene promoters and inhibition by resveratrol results in demethylation. *Proc Natl Acad Sci USA* 2012; **109**: 7765–7769.
47. Liu Y, Mayo MW, Nagji AS, Smith PW, Ramsey CS, Li D *et al*. Phosphorylation of RelA/p65 promotes DNMT-1 recruitment to chromatin and represses transcription of the tumor metastasis suppressor gene BRMS1. *Oncogene* 2012; **31**: 1143–1154.
48. Ying J, Srivastava G, Hsieh WS, Gao Z, Murray P, Liao SK *et al*. The stress-responsive gene GADD45G is a functional tumor suppressor, with its response to environmental stresses frequently disrupted epigenetically in multiple tumors. *Clin Cancer Res* 2005; **11**: 6442–6449.
49. Garcia R, Bowman TL, Niu G, Yu H, Minton S, Muro-Cacho CA *et al*. Constitutive activation of Stat3 by the Src and JAK tyrosine kinases participates in growth regulation of human breast carcinoma cells. *Oncogene* 2001; **20**: 2499–2513.
50. Chou TC. Theoretical basis, experimental design, and computerized simulation of synergism and antagonism in drug combination studies. *Pharmacol Rev* 2006; **58**: 621–681.



**Cell Death and Disease** is an open-access journal published by Nature Publishing Group. This work is licensed under a Creative Commons Attribution-NonCommercial-NoDerivs 3.0 Unported License. To view a copy of this license, visit <http://creativecommons.org/licenses/by-nc-nd/3.0/>

Supplementary Information accompanies this paper on Cell Death and Disease website (<http://www.nature.com/cddis>)